Surface phase behavior in binary polymer mixtures. III. Temperature dependence of surface enrichment and of wetting

A. Budkowski,[a] F. Scheffold, and J. Klein
Department of Materials and Interfaces, The Weizmann Institute of Science, Rehovot 76100, Israel

L. J. Fetters
Exxon Research and Engineering Company, Annandale, New Jersey 08801

Surface segregation in thin films of binary liquid mixtures consisting of random olefine copolymers was studied by nuclear reaction analysis over a wide temperature and composition range. A divergence of the surface excess Γ was indicated as the binodal of each mixture was approached from the one-phase region, even at temperatures 100 °C below the critical point T_c, and interpreted as the advent of complete wetting behavior. A consistent description of the adsorption isotherms in terms of a mean field approach assuming a short-ranged surface potential f_s is feasible, but requires an unexpected temperature dependence of f_s. This dependence causes the wetting transition temperature to be located lower than expected on the basis of present models. © *1997 American Institute of Physics.* [S0021-9606(97)51002-6]

I. INTRODUCTION

A binary liquid mixture below its critical temperature T_c consists of two coexisting phases. Where one of the phases is favored at the mixture surface it may either partially wet it, or form a macroscopic layer to exclude the other phase (complete wetting).[1-6] Mixtures of long-chain polymers provide very convenient models for the detailed study of wetting, for several reasons, as follows.[6] The complete wetting regime in such mixtures is much extended as compared to simple liquids.[3] The use of random copolymers of structure $(A_xB_{1-x})_N$ allow us to ''tune'' (via x) the average microstructure and corresponding thermodynamic interactions of the components (each with a different x value).[7,8] Here N is the degree of polymerization and A and B are structurally different monomers. Varying N also enables convenient values of T_c to be selected. Apart from providing convenient model systems, surface enrichment from polymer blends has clear technological implications for interfacial properties, and has been studied in a number of different binary systems.[9-17]

Theories of surface segregation in polymer blends have been based on the van der Waals/Cahn approach[1-3,18-20] for simple liquids. Much of the experimental data obtained so far has been successfully described by a mean-field formulation due to Schmidt and Binder[3] or by extended formulations.[6,21-26] In this formulation the equilibrium composition-depth profile near the surface of polymer blend minimizes the overall free energy. The free energy contains a (short-ranged) surface contribution f_s (generally taken as independent of temperature), as well as a term describing the bulk thermodynamics. An important prediction[3] was that the temperature range where the complete wetting occurs should not be restricted to the very narrow temperature regime close

to T_c, as is the case for simple liquids.[1,2] Indeed, complete wetting from polymer mixtures has recently been observed[12,27,28] even at temperatures some 50 °C below T_c.[28]

In earlier work we demonstrated[12,29] that complete wetting can occur in mixtures of model olefinic copolymers $(EE_xE_{1-x})_N$ where E is a linear di-ethylene (C_4H_8) group and EE is an ethylethylene $[C_2H_3(C_2H_5)]$ group. In two recent articles (parts I[8] and II[17] in this series) we extended this to the systematic investigation of such mixtures covering a range of x values. In part I we examined the miscibility and segmental interaction characteristics by determining phase coexistence diagrams (binodals) for the different pairs;[8] while in part II we investigated[17]—for the self-same mixtures—surface enrichment characteristics of the air-surface preferred phases. In these binary pairs this is always the component with the higher fraction x of branched monomers. We also examined in detail the surface segregation isotherms in two of these mixtures (at a single given temperature in each case). An analysis based on a Cahn-construction approach suggested[17] that at lower temperatures a second-order wetting transition on the coexistence curve might be observed in these mixtures.

In this third and last article of the series we study in detail the question of the temperature dependence of the surface segregation isotherms for two of the mixtures studied in parts I and II. The article is organized as follows. In Sec. II we describe the experimental details and the use of nuclear reaction analysis[30] (NRA) to determine the composition-depth profiles. In Sec. III we show the adsorption isotherms determined at different temperatures $T < T_c$ for compositions in the one-phase region of the phase diagram as they approach the binodal line. These results are analyzed in Sec. IV in terms of mean field models, and show clearly the approach to complete wetting even at temperatures far below T_c. At the same time they reveal an unexpected temperature dependence of the short-ranged surface potentials f_s assumed responsible for the surface enrichment.

[a]On leave of absence from Institute of Physics, Jagellonian University, 30059 Kraków, Poland.

TABLE I. Molecular characteristics of random copolymers $(C_4H_8)_{1-x}$-$[C_2H_3-(C_2H_5)]_x$ used in this study.

Blend	Copolymer	x	Deuteration extent e	Statistical segment length (nm)	Degree of polymerization
$d66h52$	$d66$	66	0.40	0.68	2030
	$h52$	52	$\cdots$	0.72	1510
$d86h75$	$d86$	86	0.40	0.60	1520
	$h75$	75	$\cdots$	0.64	1625

II. EXPERIMENT

Two polymer mixtures were studied, comprising four copolymers of structure $(C_4H_8)_{1-x}$-$[C_2H_3$-$(C_2H_5)]_x$, with different x values; the ethyl (C_4H_8) and ethylethylene $[C_2H_3-(C_2H_5)]$ monomers are distributed randomly on the chains. The characteristics of the copolymers are given in Table I. The pairs are $d66h52$, composed of $d66$ ($x=0.66$), which is partly deuterated and of $h52$ ($x=0.52$); and $d86h75$, composed of partly deuterated $d86$ ($x=0.86$) and of $h75$ ($x=0.75$). Deuterium labeling of one component in each pair (to an extent e denoted in Table I) was necessary for the composition profiling method (NRA) described below.

Samples of the required compositions were prepared by spin coating a film (of thickness 300–1000 nm) from toluene on a gold-covered silicon wafer ($\sim 2 \times 1$ cm^2). The samples were annealed in a vacuum oven (10^{-2} Torr) at temperatures in the range 99–184($\pm$0.5) °C. Following this the samples were quenched and stored at temperature below their glass transition temperatures T_g (~ -50 °C) until their composition-depth profiles could be analyzed.

The composition-depth profile $\phi(z)$ of the deuterated segments was determined via NRA, described in detail earlier.[30,31] In this method a beam of charged ^{3}He particles is incident at low angle on the polymer film. The energy spectrum of scattered ^{4}He particles from the reaction ^{3}He$+^2$H$\rightarrow^4$He$+^1$H$+18.35$ MeV is measured in the forward direction, and from this the composition versus depth profile $\phi(z)$ is directly determined.

III. RESULTS

A. Phase coexistence characteristics

The binodals for the blends $d66h52$ and $d86h75$ were determined in part I,[8] and are reproduced in Figs. 1 and 2, respectively.

B. Characteristics of a surface enriched and a wetting layer

The main output of our experiments is the composition-depth profiles $\phi(z)$, from which the amount of surface segregated component may be determined as a function of bulk concentration ϕ_∞ at different temperatures. Single layers of initially uniform composition of either $d66/h52$ or $d86/h75$
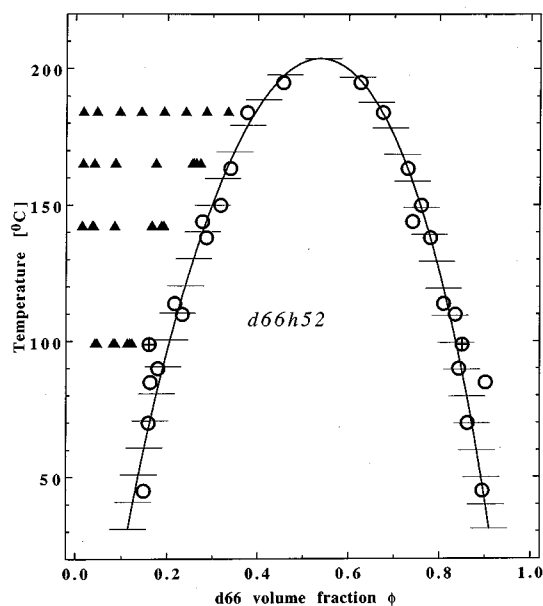

FIG. 1. The experimentally determined phase coexistence characteristics for the $d66h52$ blend (from Ref. 8): the temperature variation of coexistence concentrations ϕ_β and ϕ_α ($\bigcirc$) is described (solid line) by the interaction parameter $\chi(d66h52)=(0.327/T+3.48.10^{-4})(1+0.222\phi)$. The solid horizontal bars mark the evaluated error bars. Solid triangles ($\blacktriangle$) denote bulk equilibrium compositions ϕ_∞ for which surface excess was determined (Fig. 7). The data points denoted as ($\oplus$) correspond to the coexistence profile ($\bullet$) of Fig. 5.

were annealed to equilibrium[32] at temperatures $T<T_c$. As a result of preferential attraction of the deuterated component (with the higher ethylethylene fraction) to the free surface,[33] the profiles $\phi(z)$ were surface enriched in the deuterated
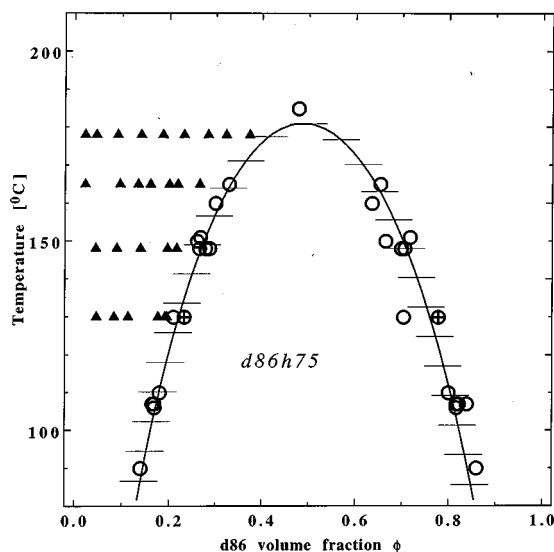

FIG. 2. The same as for Fig. 1 but for the $d86h75$ blend. The interaction parameter describing phase coexistence characteristics is now given by $\chi(d86h75)=(0.559/T+8.0.10^{-5})(1-0.057\phi)$. Solid triangles ($\blacktriangle$) denote bulk equilibrium compositions ϕ_∞ for which surface excess was determined (Fig. 8). The data points denoted as ($\oplus$) correspond to the coexistence profile ($\bullet$) of Fig. 6.
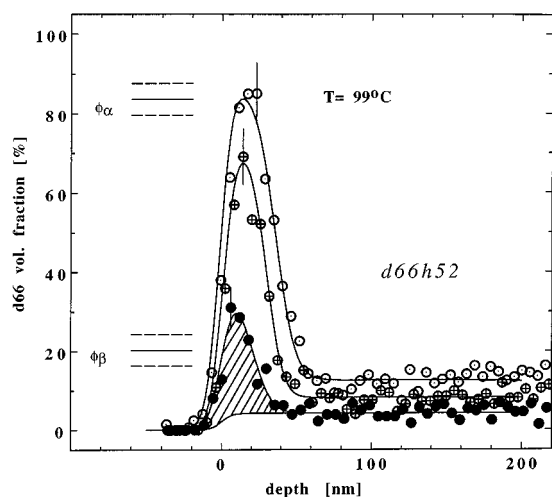
FIG. 3. Equilibrium composition-depth profiles of the $d66h52$ blend monolayers with: (●); 5% (⊕) 10%, and (○) 15% $d66$ following 2 h of annealing at 99 °C. The hatched area marks the surface excess value Γ defined in Eq. (1). The horizontal solid and dashed lines indicate the respective coexistence values ϕ_β and ϕ_α and their estimated uncertainty.

species. Figures 3–6 show characteristic profiles at different bulk concentrations. The surface excess Γ (shaded in Fig. 3) is given by

$$\Gamma = \int_0^{z(\phi_\infty)} [\phi(z) - \phi_\infty] dz. \qquad (1)$$

Here $z(\phi_\infty)$ is the distance from the surface to the plateau in composition. Γ is determined for different bulk compositions ϕ_∞ in the plateau adjacent to the surface enriched region. This is done for four different temperatures for each of the two mixtures studied; the corresponding values of ϕ_∞ are denoted as solid triangles ▲ in the $d66h52$ and $d86h75$
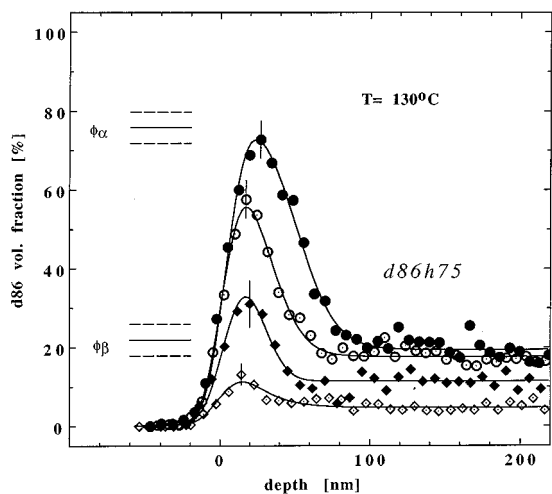

FIG. 5. Coexistence (●) and limiting surface enrichment (○) composition-depth profile of the $d66h52$ blend obtained from a 20% $d66$ and a 15% $d66$ monolayer following 15 and 2 h of annealing at 99 °C, respectively. The horizontal solid and dashed lines indicate the respective coexistence values ϕ_β and ϕ_α and their estimated uncertainty.

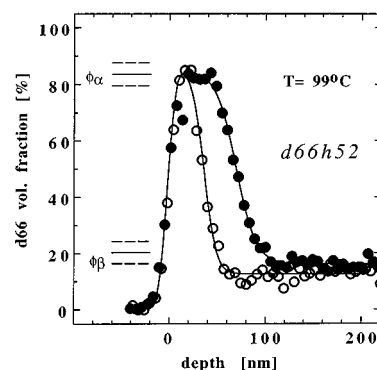phase diagrams (Figs. 1 and 2, respectively). The corresponding surface-excess isotherms are given in Figs. 7 and 8.

The shapes of the surface enriched profiles (Figs. 3 and 4) as the concentrations ϕ_∞ approach the coexistence value ϕ_β at a given temperature $T < T_c$ are revealing. The profiles shown are a convolution with the NRA depth resolution function [a Gaussian of ~8 nm half-width at half-maximum (HWHM) at the air surface] which "smear" the true composition-depth variation. Nonetheless, we may still observe (Figs. 3 and 4) that the surface concentration ϕ_s of the enriched layer attains the upper coexistence composition ϕ_α of the α phase, as ϕ_∞ approaches the lower coexistence value ϕ_β of the β phase. This is clearly seen in Figs. 5 and 6 for the limiting surface enriched profiles at $\phi_\infty < \phi_\beta$ (denoted by ○)
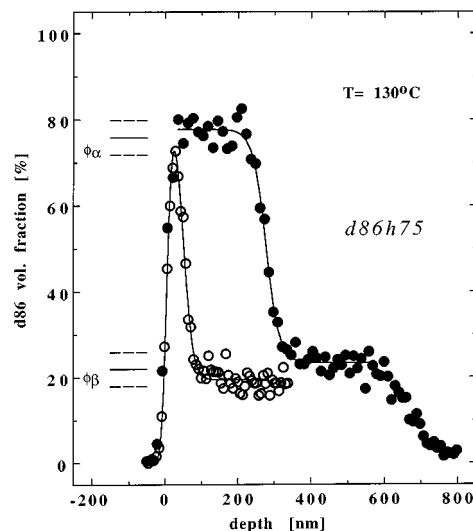

FIG. 4. Equilibrium composition-depth profiles of the $d86h75$ blend monolayers with: (◇) 5%, (◆) 12%, (☉) 22.4, and (●) 27% $d66$ following 2 h of annealing at 130 °C. The horizontal solid and dashed lines indicate the respective coexistence values ϕ_β and ϕ_α and their estimated uncertainty.

FIG. 6. Coexistence (●) and limiting surface enrichment (○) composition-depth profile of the $d86h75$ blend obtained from a $d86$ (300 nm thick)−$h75$ (360 nm-thick) bilayer following 3 h of annealing at 130 °C and from a 27% $d86$ monolayer following 2 h of annealing at 130 °C, respectively. The horizontal solid and dashed lines indicate the respective coexistence values ϕ_β and ϕ_α and their estimated uncertainty.
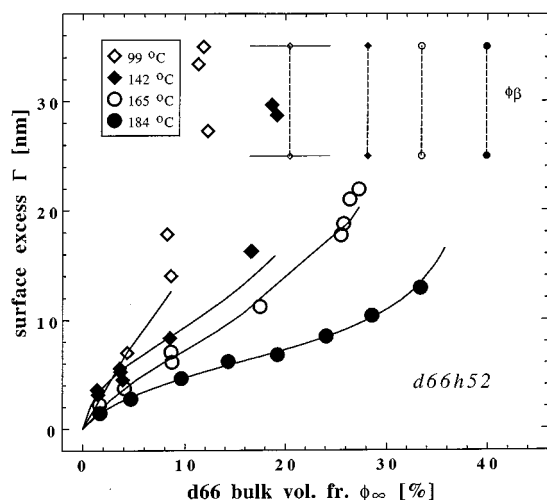
FIG. 7. Variation of the surface excess Γ at the vacuum interface of the $d66h52$ blend, as a function of a bulk volume fraction ϕ_∞, determined for different temperatures. Vertical dashed lines indicate the values of the respective coexistence compositions ϕ_β, corresponding to the different temperatures (horizontal bars are estimated uncertainties). The solid lines are mean-field predictions based on Eq. (11).

compared with the corresponding coexistence profiles (marked as ●) at $\phi_\infty = \phi_\beta$. This indicates a complete wetting regime, where there are no energetic barriers to build up a macroscopic layer of the α phase,[5] fully excluding the bulk β phase from the surface. The corresponding isotherms (Figs. 7 and 8) indicate a divergence in Γ as ϕ_∞ approaches ϕ_β, seen especially clearly for the lower temperatures studied. Within our experimental accuracy we cannot detect any discontinuity in the $\Gamma(\phi_\infty)$ dependence, which would be a characteristic of a prewetting transition.

While complete wetting on the coexistence curve in analogous mixtures has been previously reported,[12,28,29] these data show for the first time its onset on the isothermal path as the bulk concentration approaches the coexistence value. This occurs even at $T = 99$ °C for the $d66h52$ blend where

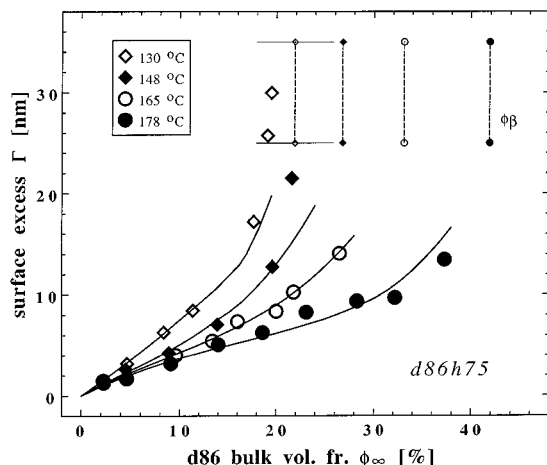FIG. 8. As Fig. 7, for the $d86h75$ blend.

$T_c = 204$ °C, and at $T = 130$ °C for the $d86h75$ blend where $T_c = 181$ °C, i.e., for $T \ll T_c$. This is in strong contrast to small-molecule liquid mixtures [where wetting takes place close to T_c (Ref. 1)], but confirms the expectations for binary polymer mixtures.[3]

IV. DISCUSSION

A. Phase coexistence and surface segregation

In the standard mean-field model, the composition profile $\phi(z)$ of the interfacial region between two coexisting polymer phases at composition ϕ_α and ϕ_β (as, for example, profiles given by the solid black points in Figs. 5 and 6) can be shown to be

$$\phi(z) = \tfrac{1}{2}[(\phi_\alpha + \phi_\beta) - (\phi_\alpha - \phi_\beta)\tanh(z/w)], \tag{2}$$

where w is an intrinsic width[34] of the interfacial region, related to the segment–segment interaction parameter χ (see captions to Figs. 1 and 2). When the same model is extended to evaluate the profiles of the surface enriched from the coexistence concentration ϕ_β in the bulk, $\phi(z)$ remains unchanged,[3] save that it is cut off at the surface by the surface concentration ϕ_s (when $\phi_s \lesssim \phi_\alpha$).

B. Characteristics of a surface enriched and a wetting layer

Two aspects of the observed surface excesses $\Gamma(\phi_\infty)$ may be analyzed within the mean-field description proposed by Cahn[1] long ago. The more general approach examines directly the surface segregation isotherms in terms of the form $\Gamma(\phi_\infty)$ expected for the complete wetting regime. Using it we may in principle distinguish partial and complete wetting regimes based on the $\Gamma(\phi_\infty)$ data. A more indirect approach, leading to the so-called Cahn construction,[1] allows us to determine the concentration derivative of the surface contribution to the free energy. It yields a certain insight into the problem of the location of the partial-to-complete wetting transition on the coexistence curve. As generally formulated and used in a number of recent studies, this latter approach assumes that the surface potentials are dominated by short-ranged fields. Below we analyze our segregation isotherm data using both approaches.

1. Analysis of surface excess isotherms

Two different types of behavior are predicted[4] for the surface excess $\Gamma(\phi_\infty)$ of the semi-infinite blend layer as the bulk concentration ϕ_∞ approaches isothermally the coexistence value ϕ_β. The excess Γ_β, obtained for ϕ_∞ equal in the limit to ϕ_β, should have a finite value for the partial wetting regime, whereas for complete wetting it should diverge to infinity. In practice the situation is more complex. Due to the finite thickness of our films Γ_β would have a finite value even in the complete wetting regime, and depends only on the overall amount of the material present in the film.

We may relate Γ_β to the concentration ϕ_s at which the coexistence profile of Eq. (2) is cut off by the polymer–air surface,
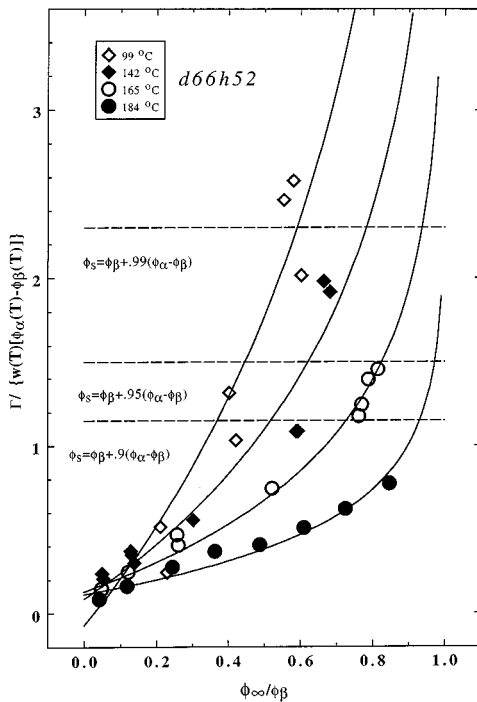
FIG. 9. The data of Fig. 7 (*d66h52*) plotted as a normalized surface excess $\Gamma/[w(\phi_\alpha-\phi_\beta)]$ vs normalized bulk volume fraction (ϕ_∞/ϕ_β). The solid lines corresponding to different annealing temperatures are according to $\Gamma/w(\phi_\alpha-\phi_\beta)\propto A'-\ln(1-\phi_\infty/\phi_\beta)$, where A' is adjusted for best fit [see Eq. (5)]. Dashed horizontal lines are normalized surface excess values for the bulk β phase enriched at the surface to the compositions ϕ_s indicated.

FIG. 10. As Fig. 9, but for *d86h75* (based on data from Fig. 8).

$$\Gamma_\beta(\phi_s) = \int_{z(\phi_s)}^\infty \left\{ \frac{1}{2}\left[(\phi_\alpha+\phi_\beta)-(\phi_\alpha-\phi_\beta) \right.\right.$$

$$\left.\left. \times\tanh\left(\frac{z}{w}\right)\right]-\phi_\beta \right\} dz$$

$$= w(\phi_\alpha-\phi_\beta)\int_{x(\phi_s)}^\infty dx\left(\frac{(1-\tanh x)}{2}\right), \tag{3}$$

where $x\equiv z/w$. Here $z(\phi_s)$ is the position where the coexistence profile has a local concentration equal to ϕ_s. In principle this is just the air surface at $z=0$, but the formulation of Eq. (3) allows a more general discussion. Surface excess values Γ_β corresponding to ϕ_s much lower than the upper coexistence value ϕ_α would indicate partial wetting. The other limit, where Γ_β corresponds to ϕ_s close to ϕ_α, would indicate the advent of the complete wetting regime.

Equation (3) suggests a convenient way of examining the segregation isotherms of Figs. 7 and 8. This is done in Figs. 9 and 10, where the temperature-dependent interfacial width w and the coexistence concentrations ϕ_α and ϕ_β are completely absorbed in the normalization of the scales. Figures 9 and 10 show how the normalized excess $\Gamma/[w(\phi_\alpha-\phi_\beta)]$ varies with the normalized concentration (ϕ_∞/ϕ_β) for the *d66h52* and the *d86h75* blends, respectively. The dashed lines marked in these figures are the normalized excess values $\Gamma_\beta/[w(\phi_\alpha-\phi_\beta)]$ obtained using Eq. (3) for the normalized difference between ϕ_α and ϕ_s, given by
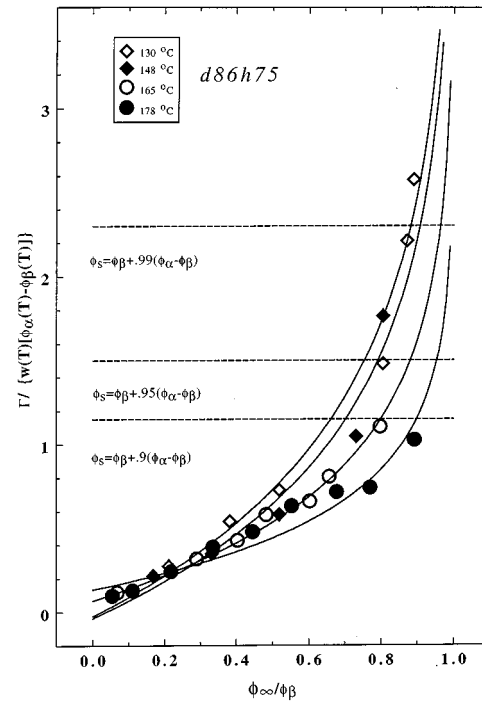
$[(\phi_\alpha-\phi_s)/(\phi_\alpha-\phi_\beta)]$, equal to 10%, 5%, and 1%, respectively. The experimental data at the lower temperatures for both blends overshoot these limits, suggesting that the complete wetting regime has been attained even for lowest temperatures of 99 and 130 °C for the *d66h52* and the *d86h75* blends, respectively. This extends our previous observation of complete wetting occurring on the coexistence curve of the *d66h52* blend at 150 °C.[28]

The thickness of the surface enriched layer at temperatures above the wetting transition was considered by Cahn.[1] For surface segregation driven by short-ranged surface fields, he predicted a logarithmic divergence of the thickness l of the surface-favored α-phase layer for bulk composition ϕ_∞ close to ϕ_β,

$$l\propto\xi_{\text{bulk}}(\phi_\alpha)[A-\ln(1-\phi_\infty/\phi_\beta)]. \tag{4}$$

Here the bulk correlation length $\xi_{\text{bulk}}(\phi_\alpha)$ is directly proportional to the intrinsic interfacial width w;[34] the constant term A may be related to the composition derivative of the surface free energy.[1] In the limit where Eq. (4) is valid close to the complete wetting limit $\phi_\infty\rightarrow\phi_\beta$ the surface excess Γ may be well approximated as $\Gamma=l(\phi_\alpha-\phi_\beta)$. Substituting $l=\Gamma/(\phi_\alpha-\phi_\beta)$, we rewrite Eq. (4) in terms of the normalized surface excess,

$$\frac{\Gamma}{w(\phi_\alpha-\phi_\beta)}\propto A'-\ln(1-\phi_\infty/\phi_\beta) \tag{5}$$

(A' may differ slightly from A due to the approximation for Γ). The solid lines of Figs. 9 and 10 were generated using Eq. (5)[43] to fit the surface excess data corresponding to the two blends at the different temperatures. While the fit is

qualitative, it is consistent with the logarithmic divergence of the segregation isotherms predicted[1] for the complete wetting regime.

2. Cahn construction analysis

We follow the standard procedure discussed in more detail in part II,[17] and reviewed recently.[6] For the case of an A/B polymer mixture confined by a surface at $z=0$, the excess free energy F per unit area of the surface may be written as

$$\frac{F}{k_B T} = f_s\left(\phi_s, \frac{d\phi_s}{dz}\right) + \int_0^\infty dz \Bigg(F_{FH}[\phi(z)]$$
$$+ \frac{a^2(\phi)}{36\phi(1-\phi)} [\nabla\phi(z)]^2 \Bigg). \tag{6}$$

Here $\phi(z)$ is the local volume fraction of the A component. $a(\phi)$ is the effective statistical segment length, related to the statistical segment lengths a_A and a_B of the two components in our mixture (see Table I) as $a^2(\phi)=(1-\phi)a^2_A+\phi a^2_B$. The first term on the right-hand side (rhs) is a bare surface contribution f_s: It is usually assumed[1,6] short ranged in the sense that it is a function only of the surface concentration ϕ_s. For generality and later discussion we include also the possibility of its dependence on the surface gradient term $(d\phi/dz)|_{z=0}$.[21,23,24] The integral represents the bulk contribution: For polymer mixtures the energy functional $F_{FH}[\phi(z)]$ is given by the standard Flory–Huggins expression,[35,36]

$$F_{FH}[\phi(z)] = \frac{\phi\ln\phi}{N_A} + \frac{(1-\phi)\ln(1-\phi)}{N_B} + \chi\phi(1-\phi)$$
$$- \Delta\mu\phi, \tag{7}$$

where N_A, N_B are the A, B degrees of polymerization and χ is the A-mer/B-mer interaction parameter; $\Delta\mu$ is the chemical potential difference.

The composition profile $\phi(z)$ from the surface $(z=0)$ to the bulk of the blend is obtained via the minimization of Eq. (6) with respect to $\phi(z)$ and ϕ_s. The composition at the surface ϕ_s $[\equiv\phi(z=0)]$ is determined in turn by the compositional derivative $(-f_1)$ of the surface free energy f_s via the following boundary condition:

$$f_1\left(\frac{\phi_s, d\phi_s}{dz}\right) \equiv -\frac{df_s}{d\phi_s} = \frac{a(\phi_s)}{3}\left(\frac{F_{FH}(\phi_s)-F_{FH}(\phi_\infty)}{\phi_s(1-\phi_s)}\right)^{1/2}$$
$$\equiv y(\phi_\infty, \phi_s). \tag{8}$$

This expression allows us to look at the surface free energy derivative $(-f_1)$ in more detail via the Cahn construction.[1] The set of points (ϕ_s, y) determines the form of f_1 in accord with Eq. (8). Since the resolution of the NRA method is not sufficient to yield directly the surface concentration values ϕ_s, we determine them based on the adsorption isotherm data $\Gamma(\phi_\infty)$ matching the mean-field predictions $\Gamma(\phi_\infty, \phi_s)$ for single ϕ_s values,
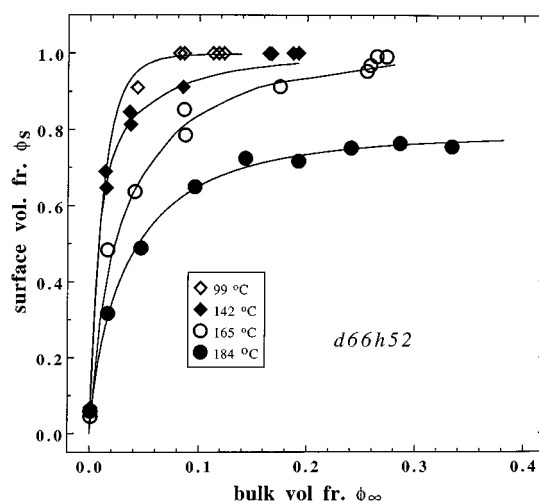

FIG. 11. The experimental adsorption isotherm data of Fig. 7 transformed using Eq. (9) into ϕ_s vs ϕ_∞ variation for the $d66h52$ blend at different temperatures. Additional points with $\phi_\infty=0.001$ are obtained by interpolation of adsorption isotherm data between (0,0) point and the lowest $\Gamma(\phi_\infty)$ value determined for each temperature. The solid lines are the mean-field predictions based on Eq. (11).

$$\Gamma(\phi_\infty, \phi_s) = \frac{1}{6}\int_{\phi_\infty}^{\phi_s} \frac{a(\phi)(\phi-\phi_\infty)d\phi}{\sqrt{\phi(1-\phi)[F_{FH}(\phi)-F_{FH}(\phi_\infty)]}}. \tag{9}$$

In this way all the adsorption isotherm $\Gamma(\phi_\infty)$ data determined at four different temperatures for both mixtures (see Figs. 7 and 8) are transformed into the concentration pairs (ϕ_∞, ϕ_s) shown in Figs. 11 and 12. For both blends, and at all temperatures, the surface concentration ϕ_s grows monotonically with bulk composition ϕ_∞ to values higher than the upper coexistence value ϕ_α, indicating the complete wetting limit.

For each concentration pair (ϕ_∞, ϕ_s) (of Figs. 11 and 12) the value of y [rhs of Eq. (8)] was calculated. Finally, sets of (ϕ_s, y) points are shown in the Cahn constructions of Figs.
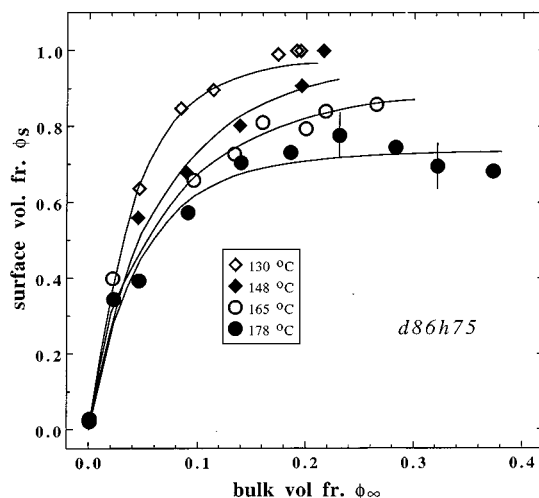

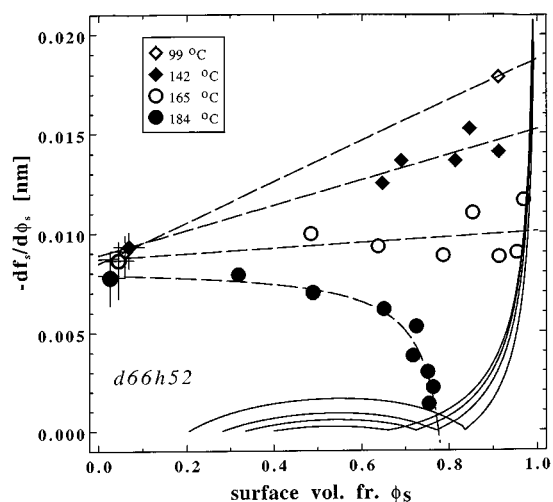FIG. 12. As Fig. 11, but for $d86h75$ (data from Fig. 8).

FIG. 13. The Cahn construction for the surface enrichment at the vacuum interface of the $d66h52$ blend. Sets of points (ϕ_s, y) were deduced via Eq. (8) from the compositional pairs (ϕ_∞, ϕ_s) of Fig. 11. They are fitted by dashed lines, expressing the compositional derivative f_1^a of the augmented surface potential f_s^a [Eq. (10)]. The solid lines are the $y(\phi_\infty, \phi_s)$ functions for $\phi_\infty = \phi_\beta$ at different temperatures. Their intersections with $f_1(\phi_s)$ at concentrations higher than ϕ_α correspond to solution of Eq. (8) indicating complete wetting.

13 and 14 for the $d66h52$ and the $d86h75$ blends. We see at once that the (ϕ_s, y) loci are temperature dependent, with a marked curvature at the higher temperatures. These observations are at variance with the simplest form of the mean-field model, in which the (short-ranged) surface field is given by $f_s(\phi_s) = -\mu_1 \phi_s - (g/2) \phi_s^2$. Here μ_1 is a chemical potential
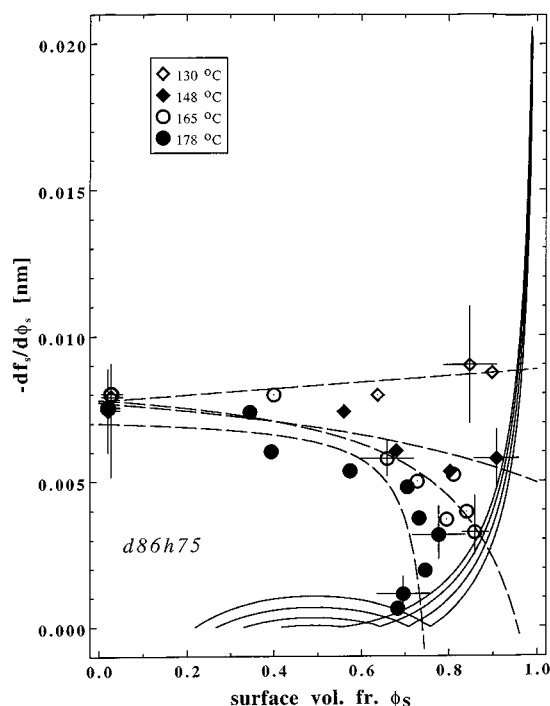

FIG. 14. As Fig. 13 but for the $d86h75$ blend (based on data from Fig. 12).

TABLE II. The surface free energy parameters used in Eq. (11), providing best fits to f_1 plots of Figs. 13 and 14.

Blend	Temperature (°C)	$\mu_{1'}$ (nm)	g' (nm)	Y' (nm²)
$d66h52$	99	0.008	0.010	0[a]
	142	0.009	0.006	0[a]
	165	0.009	0.001	0[a]
	184	0.008	−0.010	0.017
$d86h75$	130	0.008	0.001	0[a]
	148	0.008	−0.006	0.006
	165	0.008	−0.008	0.009
	178	0.007	−0.009	0.014

[a]Value fixed during fitting.

favoring one of the components at the surface, and g represents the change of interactions near the surface (''missing neighbors'' effect). The curvature of the data in Figs. 13 and 14 clearly does not fit the straight line $-\partial f_s / \partial \phi_s = \mu_1 + g \phi_s$ as pointed out already in part II.[17] There it was concluded that a better fit to the data could be obtained by adding to f_s terms linear in the gradient of the concentration profile at the surface, $d\phi_s/dz$, to give an augmented surface potential f_s^a as in Eq. (10),

$$f_s^a \left(\frac{\phi_s, d\phi_s}{dz} \right) = -\mu_1 \phi_s - \frac{g}{2} \phi_s^2 - Y \frac{d\phi_s}{dz}. \qquad (10)$$

Models incorporating such a gradient term (with different forms for Y) have been described,[6] both on entropic grounds[21,24] and as an extension to the short-range effects expected beyond nearest neighbors.[23,44] Following the approach described in part II,[17] we make use of the identity

$$\left(\frac{d\phi}{dz} \right)\bigg|_{z=0} = \left(\frac{18}{a^2} \right) \phi_s (1 - \phi_s) \frac{\partial f_s}{\partial \phi_s},$$

and find, after some algebra, the form

$$f_1^a(\phi_s) \equiv -\frac{df_s^a}{d\phi_s} = \frac{\mu_1 + g \phi_s}{1 + \dfrac{18}{a^2(\phi)} Y(1 - 2\phi_s)} = \frac{\mu_1' + g' \phi_s}{1 - \dfrac{36}{\langle a \rangle^2} Y' \phi_s}. \qquad (11)$$

With μ_1, g, and Y as adjustable parameters this yields the best-fit (dashed) lines for the different temperatures in Figs. 13 and 14. The primed surface energy parameters μ_1', g', and Y' are obtained by dividing μ_1, g, and Y by $(1 + 18Y/\langle a \rangle^2)$, where $\langle a \rangle$ is the mean statistical segment length of the blend components. These primed parameters are related more directly to the ''Cahn constructions'' of Figs. 13 and 14, since they have the correct limits at $\phi_s = 0$ (e.g., $\mu_1' = f_1^a$ for $\phi_s \rightarrow 0$). Their values, corresponding to the best fits of Figs. 13 and 14, are given in Table II.

While the question of curvature has already been examined earlier (in part II), the new feature of these experiments is the monotonic change with temperature of the f_1 loci (dashed lines in Figs. 13 and 14). These loci start at the same value μ_1' at $\phi_s = 0$, while at higher ϕ_s the dashed lines bend downward, with curvature increasing for higher

temperatures.[37] This corresponds to decreasing values of g' and increased values of Y' (Table II). Such behavior may be compared with some results[38–41] of a simple lattice theory relating the surface excess to the missing neighbor effect. According to this, the f_1 loci should be temperature dependent. The area under the $f_1(\phi_s)$ plots, being a measure of the surface tension difference between blend components, increases[40,42] for lower temperatures in accord with our experimental observations.

The final implication of the temperature variation presented in Figs. 13 and 14 concerns the nature and the location of the partial-to-complete wetting transition in these binary mixtures. As the temperature of each mixture is lowered the solid curve representing $y(\phi_\infty,\phi_s)$ shifts, so that the positions of the coexisting compositions ϕ_β and ϕ_α move out on the ϕ_s axis to lower and higher values, respectively, while at the same time the ''hump'' between them becomes bigger. If $(-df_s/d\phi_s)$—represented for each blend by the data points—were independent of temperature, then its intersection with $y(\phi_\infty,\phi_s)$ would shift smoothly to lower and lower (ϕ_s/ϕ_α) ratios as T drops and, in particular, at the lowest T measured, to $\phi_s<\phi_\alpha$. As discussed in part II,[17] this would imply a second-order wetting transition on the coexistence curve. As seen in practice, however, the $(-df_s/d\phi_s)$ loci (dashed lines) are not temperature independent but move up at lower temperatures, preventing the complete-to-partial wetting transition from occurring. The extrapolation of this effect to even lower temperatures suggests that complete wetting from these mixtures should occur even at room temperature.

V. CONCLUSIONS

In our previous two articles we investigated bulk interactions and surface enrichment in a series of random copolymer mixtures: These have the virtue of acting as ''tunable'' molecules for model studies. The present article extends this to investigate the temperature dependence of the wetting in the self-same mixtures. Our study indicates that complete wetting behavior may be observed at temperatures more than 100 °C below T_c. This emphasizes the role of the polymer size and flexibility in enabling complete wetting over a broad temperature regime in polymeric mixtures.

The adsorption isotherms, when interpreted in terms of a mean-field approach assuming short-ranged surface interactions, reveal a strong and unexpected temperature dependence of the bare surface free energy f_s. This may substantially lower the location of the wetting transition relative to T-independent surface potentials, as is seen for the two model binary mixtures studied. The suggestion is that models based on short-ranged surface potentials that seek more realistic predictions of the wetting transition in polymer mixtures should allow for such a dependence.

ACKNOWLEDGMENTS

[1] J. W. Cahn, J. Chem. Phys. **66**, 3667 (1977).
[2] P.-G. de Gennes, Rev. Mod. Phys. **57**, 827 (1985).
[3] I. Schmidt and K. Binder, J. Phys. (Paris) **46**, 1631 (1985).
[4] S. Dietrich, in *Phase Transitions and Critical Phenomena*, edited by C. Domb and J. Lebowitz (Academic, Orlando, 1988), Vol. 12, p. 1.
[5] M. Schick, in *Les Houches, Session XLVIII, Liquids at Interfaces*, edited by J. Charvolin, J. F. Joanny, and J. Zinn-Justin (North-Holland, Amsterdam, 1990), pp. 419–497.
[6] See K. Binder, Acta Polym. **46**, 204 (1995) for a recent comprehensive review.
[7] E. Eiser, A. Budkowski, U. Steiner, J. Klein, L. J. Fetters, and R. Krishnamoorti, ACS PMSE Proc. **69**, 176 (1993).
[8] F. Scheffold, E. Eiser, A. Budkowski, U. Steiner, J. Klein, and L. J. Fetters, J. Chem. Phys. **104**, 8786 (1996).
[9] Q. S. Bhatia, D. H. Pan, and J. Koberstein, Macromolecules **21**, 2166 (1988).
[10] R. A. J. Jones, E. J. Kramer, M. H. Rafailovich, J. Sokolov, and S. Schwartz, Phys. Rev. Lett. **62**, 280 (1989).
[11] X. Zhao, W. Zhao, M. H. Rafailovich, J. Sokolov, S. A. Scharz, B. J. Wilkens, R. A. L. Jones, and E. J. Kramer, Macromolecules **24**, 5991 (1991).
[12] U. Steiner, J. Klein, E. Eiser, A. Budkowski, and L. J. Fetters, Science **258**, 1126 (1992).
[13] A. Budkowski, U. Steiner, and J. Klein, J. Chem. Phys. **97**, 5229 (1992).
[14] F. Bruder, and R. Brenn, Europhys. Lett. **22**, 707 (1993).
[15] B. Guckenbiehl, M. Stamm, and T. Springer, Colloids Surf. A **86**, 311 (1994).
[16] J. Genzer, A. Faldi, R. Oslanec, and J. Composto (unpublished).
[17] F. Scheffold, A. Budkowski, U. Steiner, E. Eiser, J. Klein, and L. J. Fetters, J. Chem. Phys. **104**, 8795 (1996).
[18] J. D. Van der Waals, Z. Phys. Chem. **13**, 657 (1894).
[19] J. Cahn and J. Hillard, J. Chem. Phys. **28**, 258 (1958).
[20] H. Nakanishi and P. Pincus, J. Chem. Phys. **79**, 997 (1983).
[21] S. Cohen and M. Muthukumar, J. Chem. Phys. **90**, 5749 (1989).
[22] Z. Y. Chen, J. Noolandi, and D. Izzo, Phys. Rev. Lett. **66**, 727 (1991).
[23] R. A. Jerry and E. B. Nauman, J. Colloid Interface Sci. **154**, 122 (1992).
[24] G. H. Fredrickson and J. P. Donley, J. Chem. Phys. 8941 (1992).
[25] R. A. L. Jones, Phys. Rev. E. **47**, 1437 (1993).
[26] J. Genzer, A. Faldi, and R. J. Composto, Phys. Rev. E **50**, 2373 (1994).
[27] F. Bruder and R. Brenn, Phys. Rev. Lett. **69**, 624 (1992).
[28] U. Steiner, J. Klein, and L. J. Fetters, Phys. Rev. Lett. **72**, 1498 (1994).
[29] U. Steiner, E. Eiser, A. Budkowski, L. J. Fetters, and J. Klein, Ber. Bunsenges. Phys. Chem. **98**, 366 (1994).
[30] U. K. Chaturvedi, U. Steiner, O. Zak, G. Krausch, G. Schatz, and J. Klein, Appl. Phys. Lett. **56**, 1228 (1990).
[31] J. Klein, Science, **260**, 640 (1990).
[32] The annealing times used are sufficient to reach equilibrium, due to large diffusion coefficients D. [A. Losch, R. Salomonovic, U. Steiner, L. J. Fetters, and J. Klein, J. Polym. Sci. **33**, 1821 (1995)], e.g., the diffusion coefficient for the slowest d86 polyolefine $D=5.10^{-11}$ cm²/s allows for material diffusion in a distance of 6 μm after 2 h of annealing at 99 °C.
[33] no surface enrichment was observed at the blend interface with the gold substrate. This effect is analyzed in part II.
[34] w has been directly measured for the two couples described in this article, as well as for analogous mixtures (Ref. 7), and fits well to mean-field expressions (Ref. 6) with the appropriate χ values of Figs. 1 and 2. In this article w has been calculated numerically for each considered temperature based on the extremal value of the concentration gradient $d\phi/dz$ along the profile $\phi(z)$, using Eqs. (3.14) and (2.3) of H. Tang and K. F. Freed, J. Chem. Phys. **94**, 6307 (1991).
[35] P. J. Flory, *Principles of Polymer Chemistry* (Cornell University Press, Ithaca, NY, 1975).
[36] P.-G. de Gennes, *Scaling Concepts in Polymer Physics* (Cornell University Press, Ithaca, NY, 1979).
[37] We note also that the set of (ϕ_s,y) points determined for the d86h75 mixture at the highest temperature (178 °C Fig. 14) bears some resemblance to the branched $f_1(\phi_s)$ curve observed earlier in a different polymer mixture (Ref. 14). While the deviation of our data from the fit based

on Eq. (11) is within the scatter inherent in the data, we cannot completely exclude such scenario in our case.

[38] R. A. L. Jones, Polymer **35**, 2160 (1994).

[39] A. Hariharan and S. K. Kumar, Macromolecules **24**, 4909 (1991).

[40] R. A. Jerry and E. B. Nauman, Phys. Lett. A **167**, 198 (1992).

[41] P. Cifra, F. Bruder, and R. Brenn, J. Chem. Phys. **99**, 4121 (1993).

[42] S. K. Kumar, H. Tang, and I. Szleifer, Molecular Phys. **4**, 867 (1994).

[43] We note that Eq. (5) applies best when the inflection point is along the enrichment profile, i.e., for $\phi_{\infty}/\phi_{\beta} \rightarrow 1$.

[44] There is some controversy in the literature over the correct variational method to use when f_s contains a term in $(d\phi_s/dz)$; see e.g., R. A. Jerry and E. B. Nauman, J. Chem. Phys. **97**, 7829 (1992).